Article

Bio-based membranes and nanocomposites: a sustainable innovation for potential use in wastewater

Samuel Awobifa-Olaolu¹
Adolfo Romero-Galarza¹
Rosa Idalia Narro-Céspedes¹
S. Alejandro Lozano-Morales²
Corazón Giovanna Morales-Amaya³
Francisco J. González^{1,§}

- 1 Facultad de Ciencias Químicas-Universidad Autónoma de Coahuila. Boulevard Venustiano Carranza Ing. José Cárdenas Valdés S/N, República Oriente, Saltillo, Coahuila, México. CP. 25280.
- 2 SECIHTI-Centro de Investigación en Química Aplicada. Blvd. Enrique Reyna Hermosillo #140, Col. San José de los Cerritos, Saltillo, Coahuila, México. CP. 25294.
- 3 Centro de Investigación en Química Aplicada. Blvd. Enrique Reyna Hermosillo # 140, Col. San José de los Cerritos, Saltillo, Coahuila, México. CP. 25294.

Autor para correspondencia: fgonzalezgonzalez@uadec.edu.mx.

Abstract

Currently, the pollution generated by the textile industry in the area of dyes is a major concern at the national and international levels. One of the proposals to mitigate this problem is membrane technology. In particular, those based on composite materials and polymers of a biodegradable nature have been the subject of study in recent decades as a replacement for conventional polymer-based membranes for water treatment, due to the growing demand for sustainable technologies for this application. This work addresses the preparation and use of polymeric nanocomposites using polylactic acid and titanium dioxide (TiO₂) nanoparticles for their application as biodegradable membranes. The addition of these nanoparticles in the polymer matrix improves thermal stability and provides photocatalytic properties, allowing the removal of dyes, with potential application for wastewater treatment.

Keywords:

biodegradable polymers, dye removal, photodegradation.



License (open-access): Este es un artículo publicado en acceso abierto bajo una licencia Creative Commons

elocation-id: e4052

1



Introduction

Access to clean water is fundamental to development and human health. Nevertheless, human activity has altered water quality, and the search for solutions in this area is one of the main concerns on a global scale (Zhang *et al.*, 2022; Mojiri *et al.*, 2023). Among some of the pollutants in water, there are complex chemicals and ionizing agents that are widely used as dyes (Kumar *et al.*, 2022).

One of the factors that limits the decomposition of these dyes when they are released into wastewater is the light-refracting chemicals that hinder the natural decomposition and degradation of these compounds (Blanchard and Mekonnen, 2022; Mahmood *et al.*, 2022). In recent years, polymeric membranes have received considerable interest in solving various environmental problems, such as contaminant removal, gas separation, and water purification. Their versatility of morphology and chemical structure makes them an excellent technology for various applications in environmental sciences.

The advancement of these depends on the manufacture of membranes with high permeability and selectivity, resistance to dirt, and stability in aggressive environments. Membrane manufacturing methods have evolved over the past ten years, adopting processes that allow the porosity, thickness, and surface characteristics of the membrane to be modified.

Methods such as phase inversion, electrospinning, layer-by-layer assembly and 3D printing are innovative manufacturing processes that have made it possible to create membranes with custom shapes and functionalities and improve their performance (Zhang *et al.*, 2022; Thiam *et al.*, 2022; Ren *et al.*, 2023; Karki *et al.*, 2024; Luo *et al.*, 2024; Wang and Wei, 2024).

In addition, the performance of polymeric membranes has been increased by functionalization techniques, such as surface modification, addition of functional nanomaterials, polymer mixing, and compound formation, which allow for selective separation, antifouling properties and greater mechanical stability (Kim *et al.*, 2022). These characteristics, together with a longer useful life, good mechanical, thermal, and chemical stability, low cost, and minimal maintenance, have made them a new and promising method for wastewater treatment (Mansoori *et al.*, 2020).

One of the most promising materials for the manufacture of new polymeric membranes is polylactic acid (PLA). Due to its qualities, such as durability, mechanical strength, and transparency, PLA has established itself as one of the most promising biodegradable polymers in various industries, such as packaging, automotive, and agriculture. It is a hydrophobic polymer due to the -CH₃ side groups present in its chemical structure. In addition, it is resistant to hydrolysis due to the steric shielding effect of the methyl side groups.

PLA is obtained from the lactic acid (LA) monomer, a linear aliphatic thermoplastic polyester. LA exists in two forms, L-LA and D-LA, which are mirror-image isomers of each other due to the asymmetric carbon atom in their molecule. Their physicochemical characteristics are similar; the only distinction lies in the rotation of chemically generated plane-polarized light (Jem and Tan, 2020; Taib *et al.*, 2023). However, stereochemistry, as well as the distribution and proportion of L-LA and D-LA, directly influences the mechanical and thermal characteristics of the polymer, molecular weight, and degradation time.

For example, poly (D, L-lactide) (PDLLA) is an amorphous polymer, whereas the polymer obtained from L-LA is semicrystalline (Yuanfeng and Farmahini, 2016; Taib *et al.*, 2023). In the case of semicrystalline PLA, this polymer is mainly composed of L-LA blocks. A very relevant property of polymeric materials is the glass transition temperature (Tg), which indicates the temperature at which the amorphous areas of PLA polymers soften from their glassy state. Tg ranges from 50 to 70 °C for both amorphous and semicrystalline PLAs.

The present work studied the effect of TiO₂ incorporation into the PLA membrane on the photocatalytic performance in the degradation of methylene blue (MB). To this end, membranes based on polymeric nanocomposites with different concentrations of TiO₂ were prepared using the phase inversion method. The materials were characterized by Fourier-transform infrared (FTIR), X-ray diffraction (XRD), thermogravimetric analysis (TGA), differential scanning calorimetry (DSC), and scanning electron microscopy (SEM). The physicochemical properties of the materials were related to the photocatalytic activity in the degradation of MB at room temperature under UV light.

Materials and methods

Preparation of polymeric nanocomposites of PLA/TiO₂

The PLA used was provided by Prospector and obtained from IngeoTM 3001D. Titanium oxide (TiO₂) particles were synthesized following the reported methodology (Romero-Galarza et al., 2014). All solvents used were of high purity. The synthesis of PLA membranes by the phase inversion method was performed by dissolving 1.5 g of PLA pellets in 10 ml of N, N-dimethylformamide (DMF), stirring at 250 rpm at a temperature of 120 °C for 20 min to obtain a homogeneous mixture of the solution.

The solution was poured onto a glass plate before being placed in a coagulation bath for 24 h. To prepare the membrane with TiO_2 , the same procedure was performed by adding a certain amount of TiO_2 , 1% (15 mg), 2% (30 mg) and 4% (60 mg) by weight, to the solution under the same experimental conditions.

Characterization techniques

The SEM micrographs of the membranes were obtained with a JEOL JSM-7401F equipment. For FTIR analysis, a Nicolet iS10 device with a universal attenuated total reflectance (UATR) accessory was used. IR spectra were measured in a range of 4 000 cm⁻¹ to 400 cm⁻¹ with a resolution of 4 cm⁻¹ and 30 scans. The analysis of membrane crystallinity was performed by XRD with an X PanAnalytical Empyrean equipment with Cu k α radiation (λ = 1.54 Å) in a range of 10°-80°, at a scanning speed of 0.026° s⁻¹.

The thermal stability of the membrane was determined through TGA with a Perkin Elmer Pyris 8000 device at a heating rate of 20 °C min. The samples were scanned in a temperature range of 30 °C to 800 °C, using nitrogen as purge gas. The thermal properties of the membrane were determined by differential scanning calorimetry with a Perkin Elmer Diamond DSC, from -5 °C to 200 °C, at a heating rate of 10 °C min, maintained for 1 min at 200 °C and cooled from 200 °C to -5 °C at a cooling rate of 10 °C min, maintained for 1 min at -5 °C, and a second heating from -5 °C to 200 °C at 10 °C min, the entire analysis in a gaseous nitrogen atmosphere.

The curves shown correspond to the second heating. The glass transition temperature (Tg) and the melting temperature (Tm) were determined according to the DSC results. The degree of crystallinity (Xc) was estimated by the value of the enthalpy of fusion, according to the following equation:

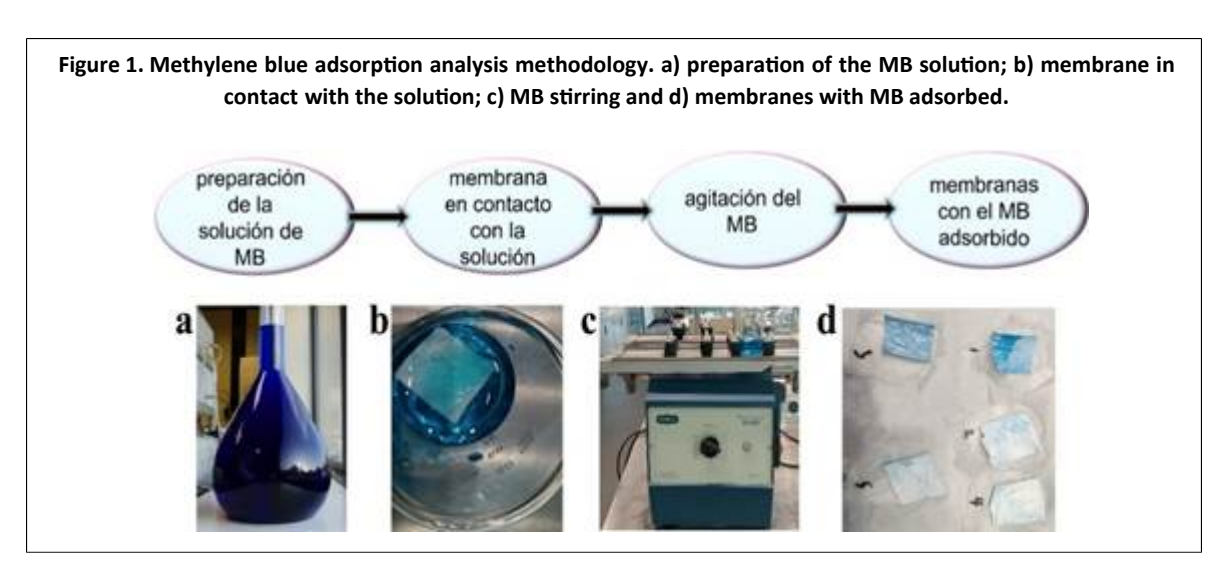
$$Xc = \frac{\Delta Hm}{\Delta H^0 m} \times 100$$

1). Where: #Hm and Δ #H Δ m represent the experimentally obtained enthalpy of fusion and that of 100% crystalline PLA, respectively, the latter with a value of 93 J g⁻¹ (Carmona *et al.*, 2015).

Analysis of MB adsorption under visible radiation

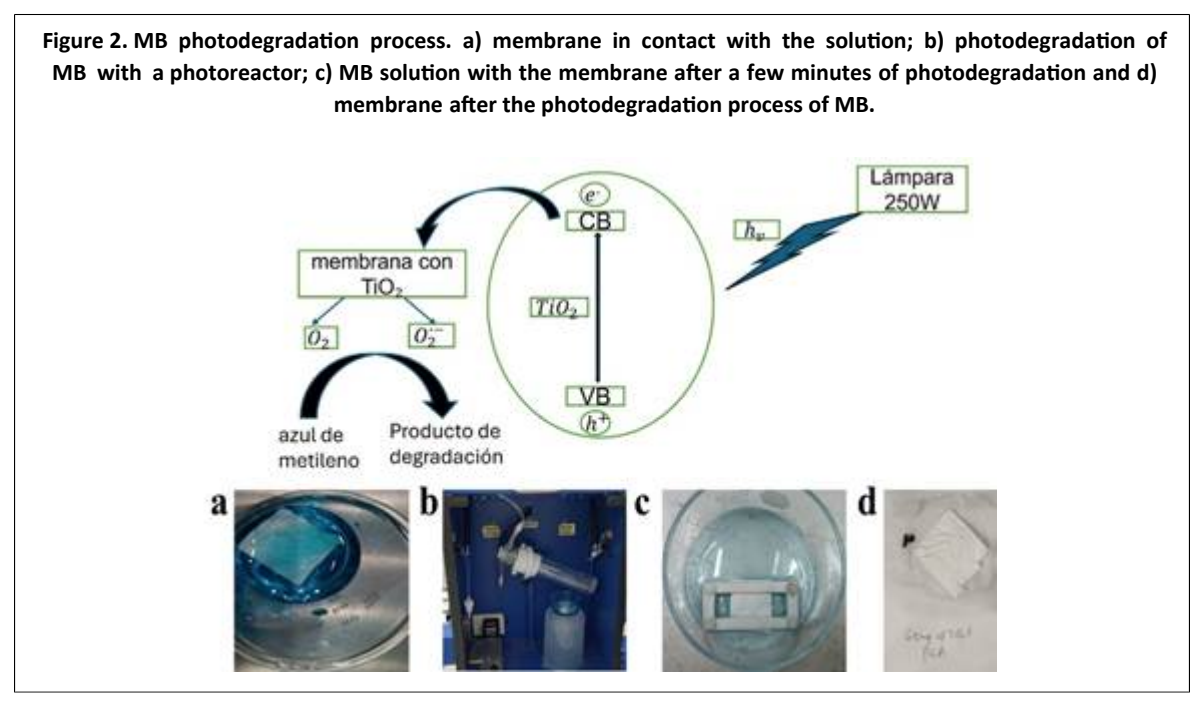
To perform the measurements of methylene blue adsorption by the membrane, it was cut into a square shape measuring 3×3 cm and placed inside the crucible with 50 ml of an aqueous solution of 5 ppm MB under continuous stirring. Aliquots of the dye solution were taken every 10 min until 80 min was reached.

The aliquots were measured with a HACH DR6000 UV-vis spectrophotometer with a reference beam optical system, scanning speed of 900 nm min⁻¹, recording data each nm, using a tungsten (370-1 100 nm) and deuterium (190-370 nm) lamp as a source. The measurement range was from 400 nm to 850 nm, and the methodology is represented in Figure 1.



Tests of photolysis and photocatalytic degradation of MB

For the tests of photolysis and photodegradation of MB, in a similar way to the tests described above. First, for photolysis tests, 50 ml of solution (5 ppm) was measured and poured into the crucible without the membrane suspended. An irradiation of 250 W of UV light (254 nm) was applied using a photoreactor for 80 min. Aliquots were taken after 10 min and measured with a UV-Vis spectrophotometer under the same conditions as the measurements in the previous section at a λ max = 665 nm. The same procedure was followed for the photodegradation of MB, but with the membrane inside the solution, as shown in Figure 2.



Results and discussion

Using SEM microscopy, it was possible to identify the porosity of the membrane and the incorporation of nanoparticles on its surface. The morphology of membranes prepared with PLA and PLA/TiO₂ is shown in the micrographs of Figure 3. In Figure 3a, it was observed that pure PLA presents a morphology consisting of a dense surface layer supported by a more porous inner sublayer.

Figure 3. a) SEM micrographs of PLA; b) and PLA/TiO₂ membranes at 1%; c) 2%; d) 4% by weight.

This is due to the phase inversion method, which allows for the movement of PLA polymer molecules and the formation of a porous membrane during the process (George *et al.*, 2024). Figure 3b-d shows the morphology of the membranes formed by PLA/TiO₂ nanocomposites at various concentrations of TiO₂. In the micrographs, it was observed that there is an agglomeration of the TiO₂ nanoparticles in the membrane.

This effect is known to affect blocking membrane pores as the concentration of TiO_2 nanoparticles increases (Hickman *et al.*, 2018; George *et al.*, 2024). FTIR spectroscopy was used to characterize the chemical structure and functional groups of both the pure membrane and the membranes of the nanocomposites, as shown in Figure 4.

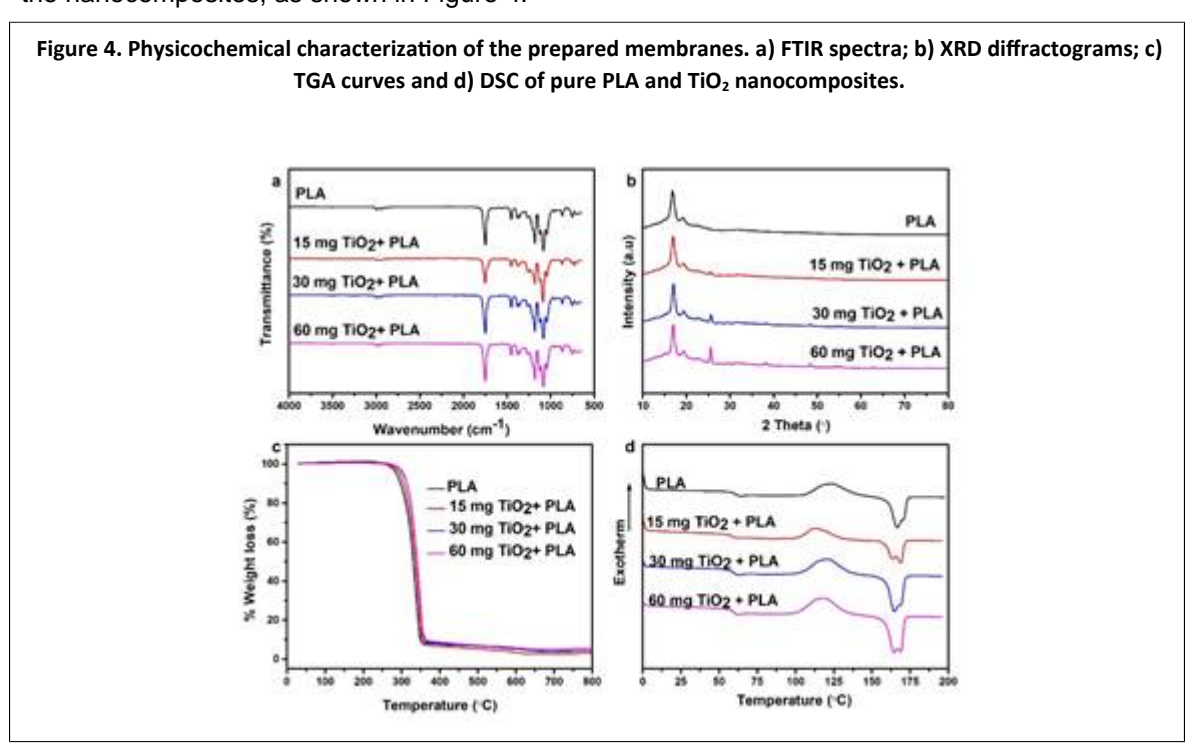




Figure 4a presents the FTIR spectra of PLA and TiO_2 -prepared materials. In the graph shown, the asymmetrical and symmetrical stretching vibrations of the C-H and CH_3 bonds are represented by the bands at 2 995 cm⁻¹ and 2 948 cm⁻¹. The C= O stretching vibration of the PLA ester group is attributed to the band at 1 750 cm⁻¹. On the other hand, the characteristic bands of the symmetrical and asymmetric deformation of -CH₃ are bands at 1 453 and 1 378 cm⁻¹.

The stretching vibration of the C-O-C bond is attributed to the band located at 1 187 cm⁻¹, while the symmetrical and asymmetric deformation of C-H corresponds to the 1 381 and 1 360 cm⁻¹ bands. The three bands between 1 044 cm⁻¹ represent the stretching vibrations of the C-O-C bonds, at 870 cm⁻¹ for the C-C bond, and the oscillating vibration of the -CH₃ group appears at 954 cm⁻¹. Finally, the bands assigned to the amorphous and crystalline phases of PLA appear at 870 cm⁻¹ and 754 cm⁻¹ (González *et al.*, 2018; Furukawa *et al.*, 2005; Salahuddin *et al.*, 2020).

It is noteworthy that the addition of TiO₂ nanoparticles does not have a noticeable effect on band position and intensity when comparing the spectra of the nanocomposite membranes and the spectrum of pure PLA. The crystallinity of pure PLA and nanocomposites was analyzed by XRD, as illustrated in Figure 4b. The graph shows the spectra with the crystalline peaks of pure PLA and different concentrations of TiO₂ nanoparticles. The diffractogram of pure PLA shows two distinctive peaks at 16.8° and 19.2°, corresponding to the reflection of the planes (200) and (203) (Inai *et al.*, 2005; Thomas *et al.*, 2020).

Likewise, from the diffractogram, the composite membrane presented a pattern of XRD that confirmed the presence of PLA with the two peaks mentioned above and TiO_2 (anatase phase) in the composite membrane. The values of 2# of the peaks obtained from the PLA of the composite membrane appear at 17° and 19.3°, and the rest of the peaks found at 25.6°, 38°, 48.3°, 54.3°, and 55.3° correspond to the anatase phase of TiO_2 .

Although the FTIR analysis showed no evidence of the presence of TiO₂, XRD was able to confirm the presence of the nanoparticles in all membranes. It is also observed that the intensity of the characteristic peaks increases with the increase in the concentration of the nanoparticles. This has already been observed by other authors, which confirms the incorporation of nanoparticles into the composite material (Mhlanga and Ray, 2014; Hou *et al.*, 2018).

TGA analysis was used to identify and quantify the thermal stability of the prepared materials. The TGA curves are represented in Figure 4c, in which a degradation process is identified in a single stage. This occurs from 282 °C to 351 °C in pure PLA, from 287 °C to 358 °C for material with 1 wt. % TiO₂, from 291 °C to 360 °C for 2 wt.%, and from 291 °C to 365 °C for 4 wt.% TiO₂.

On the other hand, the remaining mass at the end of the measurements corresponds to the residue of inorganic material. The figure shows that the addition of TiO₂ nanoparticles confers an improvement in thermal stability and decomposition temperature, which coincides with what has been reported by other authors (González *et al.*, 2018). As observed in Figure 4d, DSC analysis was used to determine the thermal properties and transitions of the prepared membranes.

Table 1 shows the data obtained from DSC, such as the glass transition temperature (Tg), the melting temperature (Tm), and the cold crystallization temperature (Tcc). Due to the characteristic melting and recrystallization behavior of PLA, both pure PLA and nanocomposites exhibit two melting peaks, the first at a temperature of 166.4 °C for PLA and at a slightly lower temperature for the rest of the materials with TiO₂. The second peak occurs due to the recrystallization and melting of the crystals formed during the DSC heating process, which has already been observed previously by other authors (Sarasua *et al.*, 1998; Teamsinsungvon *et al.*, 2022).



Table 1.	Table 1. Thermal properties of pure PLA and nanocomposites obtained through DSC.								
Sample	T _g (°C)	T _{m1} (°C)	T _{m2} (°C)	T _{cc} (°C)					
PLA	62.4	166.4	170.6	122.6					
15 mg TiO ₂ + PLA (1 wt. %)	60.8	163.6	168.8	112.8					
30 mg TiO ₂ + PLA (2 wt. %)	62.1	164.8	168.8	120.1					
60 mg TiO ₂ + PLA (4 wt. %)	61.8	164.5	168.8	117.4					

As mentioned in this paragraph, the addition of TiO_2 nanoparticles has a slight effect on the melting temperature of PLA, suggesting that these particles do not significantly affect the arrangement of the macromolecular chains of the polymer and their crystallinity under the same processing conditions, which is consistent with what other authors have reported (Liu *et al.*, 2013; Wang *et al.*, 2013; Gonzalez *et al.*, 2018).

MB adsorption tests

Figure 5 shows the UV-Vis spectra whose absorbance corresponds to the adsorption of methylene blue by the membranes and Table 2 shows the % of MB adsorption. The results obtained show that PLA experiences the highest percentage of adsorption, degrading 69.4% at 80 min, which is much higher than membranes prepared from nanocomposites, which, in the best case, achieve an adsorption of 14.97%. This behavior is due to the porous nature of PLA membranes, which was confirmed by the micrographs presented above.

Figure 5. UV-Vis spectra representing MB adsorption at different times for PLA and TiO₂ membranes: a) PLA; b) 15 mg TiO₂+PLA; c) 30 mg TiO₂+PLA and d) 60 mg TiO₂+PLA. 15 mg TiO2+ PLA 10 min Absorbance (a.u.) 20 min 20 min 30 min 50 min 60 min 70 min Wavelength (nm) 30 mg TiO2+PLA 0 min 60 mg TiO2+PLA - 10 min - 20 min 10 min Absorbance (a.u.) sorbance (a.u.) 20 min 30 min 30 min 40 min 40 min 50 min 60 min 50 min 60 min 70 min 70 min Wavelength (nm)





Adsorption (%) PLA 0 30.9 \pm 9.5 33.7 \pm 8.1 33.4 \pm 7.8 28.1 \pm 8.2 30.6 \pm 7.5 35.8 \pm 8.6 54.3 \pm 15 mg 0 18.8 \pm 3.9 5.52 \pm 1.2 0 \pm 0.2 1iO ₂ + PLA (1 wt. %)		70 54.3 ±12	60	50	40					Sample
PLA 0 30.9 \pm 9.5 33.7 \pm 8.1 33.4 \pm 7.8 28.1 \pm 8.2 30.6 \pm 7.5 35.8 \pm 8.6 54.3 \pm 15 mg 0 18.8 \pm 3.9 5.52 \pm 1.2 0 \pm 0.2 100.2 TiO ₂ + PLA (1 wt. %)		54.3 ±12			40	30	20	10	0	
15 mg 0 18.8 \pm 3.9 5.52 \pm 1.2 0 \pm 0.2 0 \pm 0.2 0 \pm 0.2 0 \pm 0.2 0 \pm 0.0 17.0 (1 wt. %)		54.3 ±12)	Adsorption (%)	,				
TiO ₂ + PLA (1 wt. %)	0.02		35.8 ±8.6	30.6 ±7.5	28.1 ±8.2	33.4 ±7.8	33.7 ±8.1	30.9 ±9.5	0	PLA
(1 wt. %)	. U ±0.2	0 ±0.2	0 ±0.2	0 ±0.2	0 ±0.2	0 ±0.2	5.52 ±1.2	18.8 ±3.9	0	15 mg
										TiO ₂ + PLA
20 0 0.02 0.02 0.02 0.02 0.02 0.02										(1 wt. %)
30 mg 0 0 ±0.2 0 ±0.2 0 ±0.2 0 ±0.2 0 ±0.2	0 ±0.2	0 ±0.2	0 ±0.2	0 ±0.2	0 ± 0.2	0 ±0.2	0 ± 0.2	0 ±0.2	0	30 mg
TiO ₂ + PLA										TiO ₂ + PLA
(2 wt. %)										(2 wt. %)
60 mg 0 8 ±2.5 9.05 ±2.8 10.3 ±3.1 5.14 ±1.6 6.55 ±2.1 8.59 ±2.7 14.7 ±	.5 15 ±4.6	14.7 ±4.5	8.59 ±2.7	6.55 ±2.1	5.14 ±1.6	10.3 ±3.1	9.05 ±2.8	8 ±2.5	0	60 mg

The addition of TiO_2 nanoparticles reduces MB adsorption, which is explained by the nanoparticles coating the pores of the composite, resulting in low adsorption values. This is evidenced in the samples with 1% and 2% by weight of TiO_2 . Nonetheless, the results suggest that at higher concentrations of TiO_2 , the effect of photodegradation begins to be observed.

Therefore, the sample with 4% by weight of TiO₂ shows a certain degree of degradation, although less than that of pure PLA. This confirms that, under visible light conditions, both mechanisms exist, although the predominant effect in prepared membranes is adsorption.

MB photodegradation tests

Figure 6 shows the UV-Vis spectrum of MB degradation when samples are exposed to UV radiation at 250 W. The results obtained from photodegradation are shown in Table 3. The results reveal an increase in the (%) of degradation, evidently due to the action of the applied radiation. In addition, a greater degradation is observed for the sample with higher TiO₂ content, since the sample with 4% by weight of TiO₂ shows a (%) degradation of 49.6% at a time of 80 min.



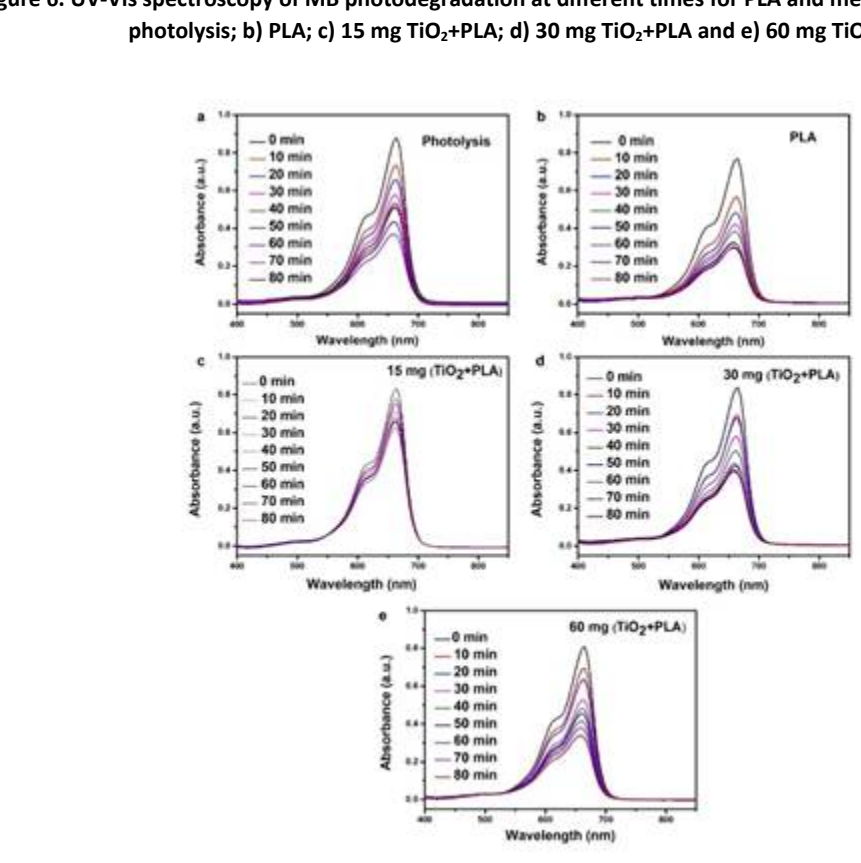


Figure 6. UV-Vis spectroscopy of MB photodegradation at different times for PLA and membranes with TiO2: a) photolysis; b) PLA; c) 15 mg TiO₂+PLA; d) 30 mg TiO₂+PLA and e) 60 mg TiO₂+PLA.

Sample	Time (min)									
	0	10	20	30	40	50	60	70	80	
				Pho	todegradation	(%)				
Photolysis	0	17.5 ±3.5	24 ±5.3	32.2 ±7.4	32.8 ±7.2	42.6 ±4.7	50 ±9.8	43.9 ±7.9	38.7 ±4.6	
PLA	0	21.2 ±2.3	32.6 ±5.9	38.1 ±4.6	41.6 ±7.1	52.1 ±9.5	49 ±9.8	50.1 ±9	44.8 ±5.4	
15 mg	0	6.06 ±1.7	8.44 ±2.1	10.7 ±4.3	14.2 ±4.2	16.5 ±1.7	19.6 ±3.9	14.8 ±2.2	15 ±2.7	
TiO ₂ + PLA										
(1 wt. %)										
30 mg	0	15.6 ±2.8	15.3 ±2.8	25.4 ±5.3	32.9 ±6.3	41.1 ±6.2	37.1 ±8.2	41.4 ±6.2	39.1 ±7	
TiO ₂ + PLA										
(2 wt. %)										
60 mg	0	12.9 ±1.9	18.5 ±2.8	29.2 ±8.8	33.7 ±6.7	36.3 ±5.1	39.7 ±4.4	43.6 ±4.8	49.6 ±7.9	
TiO ₂ + PLA										
(4 wt. %)										

As demonstrated in Figure 2, the blue coloration and intensity of the solution have decreased after the process, which is due to the catalytic effect of TiO₂ nanoparticles when exposed to UV radiation. In addition, according to the morphological characterization, the presence of TiO₂ nanoparticles uniformly distributed on the membrane surface was confirmed; these particles act as surface active sites for the photocatalytic degradation process (Deepalekshm et al., 2021; Mohammad and Atassi, 2021).



From the data presented in Table 3, with the % photodegradation of the prepared membranes, it is observed that pure PLA presents a maximum degradation of MB at 50 min. On the other hand, the membranes with TiO_2 presented a (%) of gradual degradation over time at times greater than 50 min, which implies changes in the photodegradation kinetics of the components, which depends on the concentration of TiO_2 .

Although the removal percentages are not very high, it is noteworthy that the experiments were carried out in times of up to 80 min. This contrasts with what has been reported by other authors using PLA, whose experiments are up to 12 h. This presents an advantage in terms of time-removal efficiency with the additional advantage of having a bio-based matrix, such as PLA.

The results presented in Figures 5 and 6 and Tables 2 and 3 allow us to differentiate the mechanisms, both adsorption and photocatalysis, that occur for the degradation of this dye and this type of membrane. In the case of PLA, adsorption predominates because the porous nature of the membranes allows the capture of dye molecules, and the presence of TiO₂ nanoparticles inhibits removal.

On the other hand, the photodegradation results suggest that as the concentration of TiO_2 increases, the degradation of the dye begins to occur and gradually increases as the contact time of the ultraviolet light with the solution increases. The results confirm the feasibility of using these membranes as a sustainable alternative for water treatment and removal of dyes, such as MB, for potential use in wastewater plants.

Conclusions

PLA and PLA-TiO₂ nanocomposite membranes were successfully prepared using the phase inversion method, which is a simple and easily scalable method for membrane production. The degradation capacity of the membranes was evaluated, obtaining a greater degradation by adding 4% by weight of TiO₂ nanoparticles, in a time of 80 min.

Due to the relatively high removal-time ratio and the fact that this process can be carried out in temperate environments, the membranes fabricated in the work can be used to remove dyes such as MB from industrial effluent and agricultural wastewater. Nevertheless, prospects for this research could focus on evaluating other concentrations of nanoparticles, as well as studies of pH and antibacterial properties, to proceed with the evaluation in real wastewater.

Acknowledgements

Awobifa Olaolu Samuel, with CVU: 1245789, thanks CONAHCYT, now SECIHTI, for the scholarship awarded to carry out doctoral studies, as well as the Center for Research in Applied Chemistry (CIQA) for the support and infrastructure to perform the MB degradation measurements.

Bibliography

- Blanchard, R. and Mekonnen, T. H. 2022. Synchronous pyrolysis and activation of poly (ethylene terephthalate) for the generation of activated carbon for dye contaminated wastewater treatment. Journal of Environmental Chemical Engineering. 10(6):108810. https://doi.org/10.1016/j.jece.2022.108810.
- Carmona, V. B.; Corrêa, A. C.; Marconcini, J. M. and Mattoso, L. H. C. 2015. Properties of a biodegradable ternary blend of thermoplastic starch (TPS), Poly(#-Caprolactone) (PCL) and Poly(Lactic Acid) (PLA). Journal of Polymers and the Environment. 23(1):83-89. https:// doi.org/10.1007/s10924-014-0666-7.
- Deepalekshm, P.; Yara, E.; Sabari, N. and Mohammad, H. 2021. Core-Shell nano#bers of polyvinyl alcohol/polylactic acidcontaining TiO2 nanotubes for natural sunlight drivenphotocatalysis. Macromolecular Materials and Engineering. 307(2):2100482. https://doi.org/10.1002/mame.202100482.



- Furukawa, T.; Sato, H.; Murakami, R.; Zhang, J.; Duan, Y. X.; Noda, I.; Ochiai, S. and Ozaki, Y. 2005. Structure, Dispersibility, and crystallinity of poly(hydroxybutyrate)/poly(L lactic acid) blends studied by ft-ir microspectroscopy and differential scanning calorimetry. Macromolecules. 38(15):6445-6454. https://doi.org/10.1021/ma0504668
- George, J.; Jha, S. K.; Chakrabarty, D.; Chakraborty, A. and Vaidyanathan, V. K. 2024. Superior performance of titanium coated magnetic mesoporous silica nanocomposite based poly(lactic acid) membranes for the separation of chlorophenolic organic contaminants. Journal of Polymers and the Environment . 32(5):2325-2335. https:// doi.org/10.1007/s10924-023-03098-0.
- González, E. A. S.; Olmos, D.; Lorente, M. Á.; Vélaz, I. and González-Benito, J. 2018. Preparation and characterization of polymer composite materials based on pla/tio2 for antibacterial packaging. Polymers. 10(12):1365. https://doi.org/10.3390/polym10121365.
- Hickman, R.; Walker, E. and Chowdhury, S. 2018. TiO 2 -PDMS composite sponge for adsorption and solar mediated photodegradation of dye pollutants. Journal of Water Process Engineering. 24:74-82. https://doi.org/10.1016/j.jwpe.2018.05.015.
- Hou, X.; Cai, Y.; Mushtaq, M.; Song, X.; Yang, Q.; Huang, F. and Wei, Q. 2018. Deposition of TiO2 nanoparticles on porous polylactic acid fibrous substrates and its photocatalytic capability. Journal of Nanoscience and Nanotechnology. 18(8):5617-5623. https://doi.org/10.1166/jnn.2018.15426.
- Inai, R.; Kotaki, M. and Ramakrishna, S. 2005. Structure and properties of electrospun PLLA single nanofibres. Nanotechnology. 16(2):208-213. https://doi.org/10.1088/0957-4484/16/2/005.
- Jamee, R. and Siddique, R. 2019. Biodegradation of synthetic dyes of textile effluent by microorganisms: an environmentally and economically sustainable approach. European Journal of Microbiology and Immunology. 9(4):114-118. https://doi.org/10.1556/1886.2019.00018.
- Jem, K. J. and Tan, B. 2020. The development and challenges of poly (lactic acid) and poly (glycolic acid). Advanced Industrial and Engineering Polymer Research. 3(2):60-70. https://doi.org/10.1016/j.aiepr.2020.01.002.
- Karki, S.; Hazarika, G.; Yadav, D. and Ingole, P. G. 2024. Polymeric membranes for industrial applications: recent progress, challenges and perspectives. Desalination. 573:117200. https://doi.org/10.1016/j.desal.2023.117200.
- Kim, A.; Hak-Kim, J. and Patel, R. 2022. Modification strategies of membranes with enhanced anti-biofouling properties for wastewater treatment: a review. Bioresource Technology. 345:126501. https://doi.org/10.1016/j.biortech.2021.126501.
- Kumar, V.; Thakur, C. and Chaudhari, P. K. 2022. Anaerobic biological treatment of dye bearing water in anaerobic sequencing batch reactor: performance and kinetics studies. Journal of the Indian Chemical Society. 99(10):100673. https://doi.org/10.1016/ j.jics.2022.100673.
- Liu, M.; Cheng, Z.; Yan, J.; Qiang, L.; Ru, X.; Liu, F.; Ding, D. and Li, J. 2013. Preparation and characterization of TiO2 nanofibers via using polylactic acid as template. Journal of Applied Polymer Science. 128(2):1095-1100. https://doi.org/10.1002/app.38166.
- Luo, T.; Farooq, A.; Weng, W.; Lu, S.; Luo, G.; Zhang, H.; Li, J.; Zhou, X.; Wu, X.; Huang, L.; Chen, L. and Wu, H. 2024. Progress in the preparation and application of breathable membranes. Polymers . 16(12):1686. https://doi.org/10.3390/polym16121686.
- Mahmood, K.; Amara, U.; Siddique, S.; Usman, M.; Peng, Q.; Khalid, M.; Hussain, A.; Ajmal, M.; Ahmad, A.; Sumrra, S. H.; Liu, Z.-P.; Khan, W. S.; and Ashiq, M. N. 2022. Green synthesis of Ag@CdO nanocomposite and their application towards brilliant green



- dye degradation from wastewater. Journal of Nanostructure in Chemistry. 12(3):329-341. https://doi.org/10.1007/s40097-021-00418-5.
- Mansoori, S.; Davarnejad, R.; Matsuura, T. and Ismail, A. F. 2020. Membranes based on non-synthetic (natural) polymers for wastewater treatment. Polymer Testing. 84:106381. https://doi.org/10.1016/j.polymertesting.2020.106381.
- Mhlanga, N. and Ray, S. S. 2014. Characterisation and thermal properties of titanium dioxide nanoparticles-containing biodegradable polylactide composites synthesized by Sol-Gel Method. Journal of Nanoscience and Nanotechnology . 14(6):4269-4277. https://doi.org/10.1166/jnn.2014.8271.
- Mohammad, N. and Atassi, Y. 2021. TiO2/PLLA Electrospun nanofibers membranes for efficient removal of methylene blue using sunlight. Journal of Polymers and the Environment . 29(2):509-519. https://doi.org/10.1007/s10924-020-01895-5.
- Mojiri, A.; Zhou, J. L.; Karimi-Dermani, B.; Razmi, E. and Kasmuri, N. 2023. Anaerobic membrane bioreactor (anmbr) for the removal of dyes from water and wastewater: progress, challenges, and future perspectives. Processes. 11(3):855. https://doi.org/10.3390/pr11030855.
- Ren, G.; Wan, K.; Kong, H.; Guo, L.; Wang, Y.; Liu, X. and Wei, G. 2023. Recent advance in biomass membranes: fabrication, functional regulation, and antimicrobial applications. Carbohydrate Polymers . 305:120537. https://doi.org/10.1016/j.carbpol.2023.120537.
- Romero-Galarza, A.; Dahlberg, K. A.; Chen, X. and Schwank, J. W. 2014. Crystalline structure refinements and properties of Ni/TiO2 and Ni/TiO2-Ce catalysts and application to catalytic reaction of "CO+NO". Applied catalysis a: general. 478:21-29. https://doi.org/10.1016/j.apcata.2014.03.029.
- Salahuddin, N.; Abdelwahab, M.; Gaber, M. and Elneanaey, S. 2020. Synthesis and design of norfloxacin drug delivery system based on PLA/TiO2 nanocomposites: antibacterial and antitumor activities. Materials Science and Engineering. 108:110337. https://doi.org/10.1016/j.msec.2019.110337.
- Sarasua, J. R.; Prud'homme, R. E.; Wisniewski, M.; Borgne, A. and Spassky, N. 1998. Crystallization and melting behavior of polylactides. Macromolecules . 31(12):3895-3905. https://doi.org/10.1021/ma971545p.
- Taib, N. A. A. B.; Rahman, M. R.; Huda, D.; Kuok, K. K.; Hamdan, S.; Bakri, M. K. B.; Julaihi, M. R. M. B. and Khan, A. 2023. A review on poly lactic acid (pla) as a biodegradable polymer. Polymer Bulletin. 80(2):1179-1213. https://doi.org/10.1007/s00289-022-04160-y.
- Teamsinsungvon, A.; Ruksakulpiwat, C. and Ruksakulpiwat, Y. 2022. Effects of titanium-silica oxide on degradation behavior and antimicrobial activity of poly (lactic acid) composites. Polymers . 14(16):3310. https://doi.org/10.3390/polym14163310.
- Thiam, B. G.; Magri, A. E.; Vanaei, H. R. and Vaudreuil, S. 2022. 3D printed and conventional membranes a review. Polymers . 14(5):1023. https://doi.org/10.3390/polym14051023.
- Thomas, M. S.; Pillai, P. K. S.; Faria, M.; Cordeiro, N.; Kailas, L.; Kalarikkal, N.; Thomas, S. and Pothen, L. A. 2020. Polylactic acid/nano chitosan composite fibers and their morphological, physical characterization for the removal of cadmium(II) from water. Journal of Applied Polymer Science. 137(34):48993. https://doi.org/10.1002/app.48993.
- Wang, W. W.; Man, C. Z.; Zhang, C. M.; Jiang, L.; Dan, Y. and Nguyen, T. P. 2013. Stability of poly(I-lactide)/TiO2 nanocomposite thin films under UV irradiation at 254 nm. Polymer Degradation and Stability. 98(4):885-893. https://doi.org/10.1016/j.polymdegradstab.2013.01.003.
- Wang, Y. and Wei, G. 2024. Recent trends in polymer membranes: fabrication technique, characterization, functionalization, and applications in environmental science (Part I). Polymers . 16(20):2889-. https://doi.org/10.3390/polym16202889.



- Yuanfeng, P.; Farmahini-Farahani M.; O'Hearn, P.; Xiao, H. and Ocampo, H. 2016. An overview of bio based polymers for packaging materials. Journal of Bioresources and Bioproducts. 1(3):106-113. https://doi.org/10.21967/jbb.v1i3.49.
- Zhang, H.; Li, H.; Gao, D. and Yu, H. 2022. Source identification of surface water pollution using multivariate statistics combined with physicochemical and socioeconomic parameters. Science of the Total Environment. 806:151274. https://doi.org/10.1016/j.scitotenv.2021.151274.
- Zhang, S.; Shen, L.; Deng, H.; Liu, Q.; You, X.; Yuan, J.; Jiang, Z.; and Zhang, S. 2022. Ultrathin membranes for separations: a new era driven by advanced nanotechnology. Advanced Materials. 34(21):2108457. https://doi.org/10.1002/adma.202108457.





Bio-based membranes and nanocomposites: a sustainable innovation for potential use in wastewater

Journal Information

Journal ID (publisher-id): remexca

Title: Revista mexicana de ciencias agrícolas

Abbreviated Title: Rev. Mex. Cienc. Agríc

ISSN (print): 2007-0934

Publisher: Instituto Nacional de Investigaciones

Forestales, Agrícolas y Pecuarias

Article/Issue Information

Date received: 00 July 2025

Date accepted: 00 September 2025

Publication date: 15 October 2025

Publication date: Sep-Oct 2025

Volume: 16
Issue: esp30

Electronic Location Identifier: e4052

DOI: 10.29312/remexca.v16i30.4052

Article Id (other): 00015

Categories

Subject: Articles

Keywords

Keywords

biodegradable polymers dye removal photodegradation

Counts

Figures: 6Tables: 3Equations: 0References: 34Pages: 0